Macromolecules **2000,** *33,* 877−886

Effect of Surfactant on Dynamic and Viscoelastic Properties of Aqueous Solutions of Hydrophobically Modified Ethyl(hydroxyethyl)cellulose, with and without Spacer

Anna-Lena Kjøniksen,[‡] Susanne Nilsson,[†] Krister Thuresson,[†]
Björn Lindman,[†] and Bo Nyström*,[‡]

Department of Chemistry, University of Oslo, P.O. Box 1033, Blindern, N-0315 Oslo, Norway, and
Physical Chemistry 1, Chemical Center, University of Lund, P.O. Box 124, S-221 00 Lund, Sweden

Received July 13, 1999; Revised Manuscript Received September 29, 1999

ABSTRACT: Dynamical, rheological, and some structural properties of 1 wt % aqueous solutions (semidilute regime) of ethyl(hydroxyethyl)cellulose (EHEC) and of a hydrophobically modified analogue, with (HM4-EHEC) and without (HM0-EHEC) spacer (the spacer consists of four EO groups), in the presence of various amounts of sodium dodecyl sulfate (SDS) have been investigated by different experimental methods. Both the dynamical and rheological relaxation processes were slowed at moderate surfactant concentrations due to enhanced hydrophobic associations. The time correlation data obtained from the dynamic light scattering (DLS) experiments showed the existence of two relaxation modes, one single exponential at short times followed by a stretched exponential at longer times. The slow relaxation time, as well as the rheological counterpart (the longest relaxation time), revealed an optimum in intermolecular hydrophobic interactions for the HM4-EHEC/SDS and HM0-EHEC/SDS systems at a surfactant concentration of ca. 4 m*m*, while the corresponding concentration for the EHEC/SDS system is ca. 15 m*m*. The dynamical and rheological features were found to be strongly dependent upon the level of surfactant addition, with at first an increase and then a decrease in the values of the parameters. The values are highest for the HM0-EHEC/SDS system, followed by those representing the HM4-EHEC/SDS system, and the lowest values were observed for the EHEC/SDS system. Under conditions of high association strength, the angular dependence of the slow mode of the three systems is much stronger than that of the fast diffusive mode and decreases at high SDS concentrations. This wave vector dependence of the slow relaxation time as well as other dynamic features can be rationalized in the framework of the coupling model of Ngai. At high surfactant concentrations, the influence of hydrophobic association was essentially lost, and the behavior is virtually the same for the three polymers. The picture that emerges from this study is that the associated polymer network undergoes a structural reorganization from a heterogeneous structure at low surfactant concentrations to a more homogeneous network at high levels of surfactant addition.

Introduction

Complex aqueous solutions containing hydrophobically modified polymers and surfactants receive great attention because of their practical use in a number of areas such as detergency, paints, cosmetics, oil recovery, etc.[1−4] Typically, less than 2% incorporation of the hydrophobic monomer into the polymer backbone is necessary to yield strong associative behavior. It is well established that the interaction of a nonionic polymer such as ethyl(hydroxyethyl)cellulose with an anionic surfactant such as sodium dodecyl sulfate (SDS) can induce charging effects of the polymer and in effect imparting polyelectrolyte properties to the nonionic polymer.[5] The strong polymer−surfactant interactions often manifest themselves through a significant viscosity enhancement[6−9] at a certain concentration of the surfactant. In addition to an increase in viscosity, these systems also exhibit considerable viscoelastic effects. If the hydrophobicity of the polymer is relatively high, the interactions can be enhanced to modify their rheological properties. The role of hydrophobic interactions becomes evident when the polymer contains a low fraction of very hydrophobic side groups. In aqueous solution the hydrophobic groups associate and form micellar type clusters. This association endows intriguing structural, dynamical, and rheological features to these amphiphilic polymer systems. In view of these aspects, we may argue that the behavior of polymer−surfactant mixtures is usually the result of a subtle balance between hydrophobic and hydrophilic interactions. In the presence of an ionic surfactant, the electrostatic forces will also come into play.

Recently, structural,[10] dynamical,[11] and rheological[11,12] features of aqueous solutions of a hydrophobically modified ethyl(hydroxyethyl)cellulose (HM-EHEC) (the hydrophobic modification consists of a low number of branched nonylphenol groups grafted to the polymer backbone) and an unmodified (EHEC) analogue in the presence of SDS have been reported. Both the dynamic light scattering and the rheological experiments revealed enhanced polymer−surfactant interaction for the EHEC/SDS and HM-EHEC/SDS at surfactant concentrations of 8−10 and 4−5 m*m*, respectively. The increase of the dynamic viscosity was approximately 5-fold for EHEC and 15 times for the hydrophobically modified polymer. The present investigation constitutes an extension of these studies, where a scrutiny and comparison of the characteristic features from intensity light scattering (ILS), dynamic light scattering (DLS), and rheology on aqueous solutions of EHEC (this sample is somewhat different from that used in the above investigations) and of a hydrophobically modified analogue

---

[‡] University of Oslo.
[†] University of Lund.
* Corresponding author.

10.1021/ma9911391 CCC: $19.00

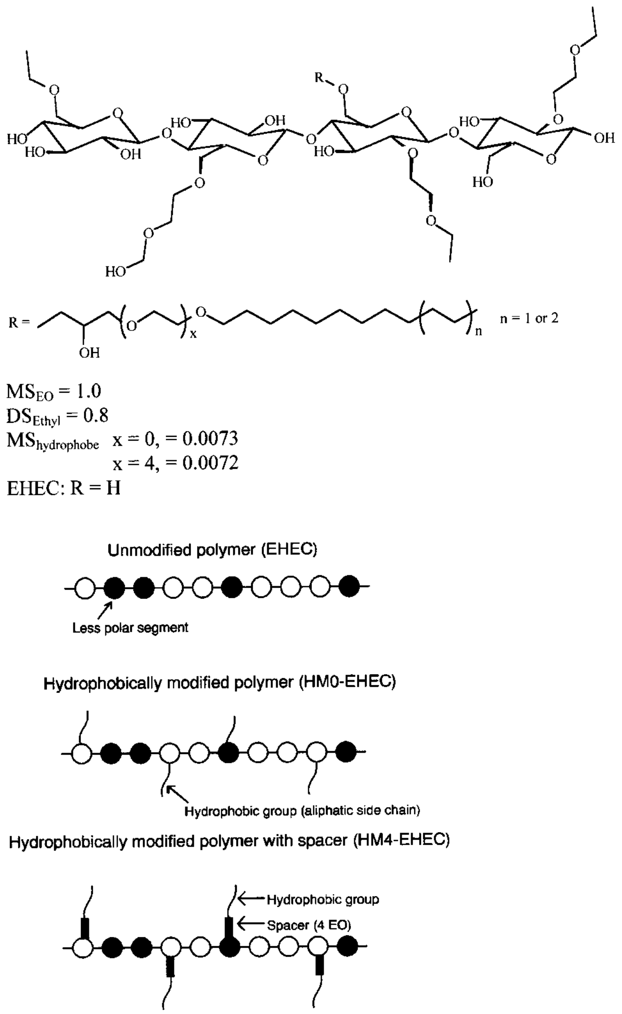

Figure 1. Structure and a schematic illustration of EHEC, HM0-EHEC, and HM4-EHEC.

(mixture of C_{12} and C_{14} alkyl chains grafted to the polymer backbone) without (HM0-EHEC) and with spacer (HM4-EHEC) in the presence of various amounts of SDS will be presented. The principal objective of this work is to investigate whether the introduction of a spacer between the polymer backbone and the polymer hydrophobic tail has any pronounced influence on the structural, dynamical, and rheological properties of this polymer in the presence of different levels of SDS addition. It is well-known that when hydrophobic moieties are attached to the polymer backbone, this effect usually gives rise to changed physical properties of the polymer–surfactant mixture; e.g., a viscosity enhancement is frequently observed as a result of the hydrophobic modification of the polymer. However, our knowledge is much more restricted when it comes to the effect of a spacer, which is incorporated in between the polymer backbone and the hydrophobic tail. In this case, when the hydrophobic tails are displaced from the polymer backbone by a flexible spacer, we may suspect that the strength of both the polymer–polymer hydrophobic interactions and the polymer–surfactant interactions should be affected. This issue is addressed in this work, and the present results yield new information about the effect of spacer on polymer–surfactant interactions.

The structure of the polymer is illustrated in Figure 1, together with a schematic illustration of the location of the hydrophobic groups and spacers on the polymer backbone. The HM0-EHEC sample consists of a mixture of C_{12} and C_{14} alkyl chains grafted to the polymer backbone, and the spacer of the spacer-containing analogue (HM4-EHEC) utilized in this work is made of four ethylene oxide groups. The surmise is that, by introducing a spacer in between the polymer backbone and the side chain, the side chain becomes more flexible. We may note that also the unmodified polymer (EHEC) possesses hydrophobicity, because it is characterized by mixed hydrophobic (ethyl groups) and hydrophilic structural units, randomly distributed along the cellulose backbone. In addition, these structural elements are normally unevenly distributed along the polymer backbone, and the substituents may consist of shorter or longer chains, giving rise to a varying degrees of hydrophobicity.

To characterize the polymer–surfactant interactions in these systems, light scattering (ILS and DLS) and oscillatory shear measurements have been carried out on semidilute aqueous solutions (at a fixed concentration of 1 wt %) of EHEC, HM0-EHEC, and HM4-EHEC in the presence of different levels of SDS addition.

Experimental Section

Materials and Sample Preparation. The three polymer samples, ethyl(hydroxyethyl)cellulose (EHEC), the hydrophobically modified analogue (HM0-EHEC), and the spacer-containing analogue (HM4-EHEC), were supplied by Akzo Nobel Surface Chemistry AB, Stenungsund, Sweden. These samples are equivalent except for a low amount of hydrophobic side chains (70% C_{12} and 30% C_{14} alkyl chains) grafted to the two modified polymers and the incorporation of spacer (made of four EO groups) of the HM4-EHEC polymer (see Figure 1). The two selected hydrophobically modified polymers have the same molar substitution of hydrophobic groups $MS_{hydrophobe}$, which refers to the average fraction of polymer repeating units that are substituted with a hydrophobic tail (see Figure 1). A value of $MS_{hydrophobe} = 0.0073$ suggests that 0.73% of the anhydroglucose units carries hydrophobic side chains. The three polymer samples have all the same average molecular weight ($M \approx 100\,000$) and degree of substitution of ethyl and hydroxyethyl groups ($DS_{ethyl} = 0.8$ and $MS_{EO} = 1.0$, respectively). The molecular weights, DS, and MS were all given by the manufacturer. In addition, intensity light scattering measurements[13] have been performed on dilute aqueous solutions of these polymers in the presence of 20 m*m* SDS (at this condition the tendency of forming aggregates in the solution is strongly suppressed), and the results suggest that the molecular weight ($M_w \approx 100\,000$) is the same for the three polymers. Prior to use, the polymers were purified as previously described.[14]

The anionic surfactant SDS was obtained from Fluka (DLS measurements) and Sigma-Aldrich (rheological measurements) and was used as received. The polymer concentration throughout this investigation is 1 wt %, which is well in the semidilute regime.[7] Samples were prepared by weighing the components, and the solutions were homogenized by stirring at room temperature for several days. All measurements were carried out at 25 °C. For light scattering measurements the solutions were filtered at room temperature through 0.8 μm filters (Micro Filtration Systems) or 5.0 μm filters (Lida), depending on the viscosity of the sample, directly into precleaned 10 mm NMR tubes (Wilmad Glass Co.) of the highest quality. Finally the tubes containing the clarified solution were sealed.

Rheological Experiments. The oscillatory shear measurements were conducted on a CarriMed CSL 100 constant stress rheometer, equipped with an automatic gap setting. Depending on the viscosity of the sample 1° acrylic cone and plate geometry with a diameter of 4 or 6 cm, respectively, was used. The oscillating sweep measurements were carried out in the approximate frequency domain 0.005−30 Hz. The values of the stress amplitude were checked in order to ensure that all experiments were performed within the linear viscoelastic regime, where the dynamic storage modulus (G') and loss modulus (G'') are independent of the applied stress. The temperature of the sample was controlled to within ±0.1 °C with the aid of a Peltier plate.

Light Scattering. In light scattering experiments we probe a wave vector $q = (4\pi n/\lambda)\sin(\theta/2)$, where λ is the wavelength of the incident light in a vacuum, θ is the scattering angle, and n is the refractive index of the medium. The value of n was determined for each sample at $\lambda = 488$ nm by using an Abbé refractometer.

We used a standard, laboratory-built light-scattering spectrometer capable of both time-average scattered intensity and photon correlation measurements. The beam from an argon ion laser (Spectra Physics model 2020), operating at 488 nm with vertically polarized light, was focused onto the sample cell through a temperature-controlled chamber (temperature controlled to within ±0.05 °C) filled with refractive-index-matching dibuthyl phthalate.

The intensity light scattering (ILS) measurements were conducted using ALV (Langen, Germany) light scattering electronics in combination with the on-line program ODIL. The ILS experiments were performed at several scattering angles, and the total scattered intensity was recorded at each angle. The interval between each angle of measurement was 2°, the duration of each measurement was 8 s, and there were six repetitions at each angle. The intensity of the output beam was adjusted with the aid of high-quality neutral density filters (Melles Griot). To ensure a vv configuration, polarizers were placed both in front and behind the cell. In the experimental setup a detection geometry was utilized where a vertical slit, instead of the usual pinhole, was placed in front of the photomultiplier tube. With this arrangement, the absolute quantity $R_{vv}(q)$, which is the excess Rayleigh ratio with vertically polarized incident and scattered beams, can be determined from the relation $R_{vv}(q) = hI^*(q)$, where $I^*(q)$ is the excess scattered intensity and $h = R_{vv,benzene}n_{solv}/(I^*_{benzene}n_{benzene})$. A value of $R_{vv}(90°) = 3.4 \times 10^{-5}$ cm^{-1} reported[15] for benzene at 25 °C and 488 nm was used in this work. The optical constant K (cm^3 mol g^{-2}) was calculated from $K = (4\pi^2n^2/N_A\lambda^4)(\partial n/\partial c)^2$, where N_A is Avogrado's constant, $\partial n/\partial c$ is the refractive index increment, and c is the mass/volume concentration. The reduced scattered intensity, $Kc/R_{vv}(q)$, was calculated from a Guiner plot[16] of $\ln(Kc/R_{vv}(q))$ versus q^2. The values of the refractive index increment for the different samples were determined with a Brice-Phoenix differential refractometer (model BP-2000-V).

In the DLS experiments, the full homodyne intensity autocorrelation function $g^2(q,t)$ was measured at different scattering angles (30−90°) with an ALV-5000 multiple tau digital correlator. If the scattered field obeys Gaussian statistics, the measured correlation function $g^2(q,t)$ can be related to the theoretically amenable first-order electric field correlation function $g^1(q,t)$ by the Siegert relationship $g^2(q,t) = 1 + B|g^1(q,t)|^2$, where B is usually treated as an empirical factor. The correlation functions were recorded in the real-time "multiple tau" mode of the correlator, in which 256 time channels were logarithmically spaced over an interval ranging from 0.2 μs to almost 1 h.

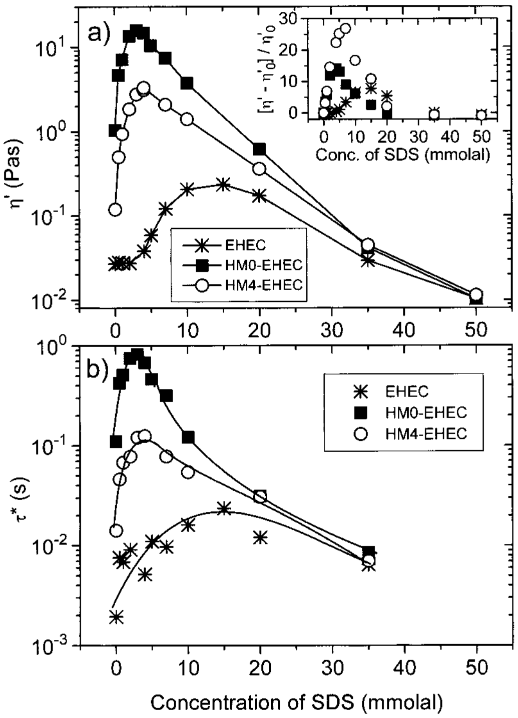

Figure 2. (a) Dynamic viscosity at 0.01 Hz as a function of SDS concentration. The inset plot illustrates the change of the dynamic viscosity from its initial value when no SDS is present (η'_0). (b) The time of intersection, τ^*, as a function of the surfactant concentration.

In the analysis of correlation functions of semidilute associating polymer solutions, one usually observes[11,17−22] a bimodal time autocorrelation function consisting of one single-exponential decay associated with cooperative diffusion ($\tau_f^{-1} = D_cq^2$, where τ_f is the "fast" relaxation time and D_c is the cooperative diffusion coefficient) in the long wavelength regime ($q\xi < 1$, where ξ is the correlation length) and a group of relaxation modes characterizing disengagement relaxation of individual chains[19,23] or cluster relaxation.[24] In this work, as well as in other DLS studies[11,20−22] on complex polymer systems, the decays of the correlation functions were throughout found to be well described by two modes: initially a single exponential, followed at longer times by a stretched exponential:

$$g^1(t) = A_f \exp(-t/\tau_f) + A_s \exp[-(t/\tau_{se})^{\beta}] \qquad (1)$$

with $A_f + A_s = 1$. This relationship is found to capture the characteristic features of the present systems. The quantities A_f and A_s are the amplitudes for the fast and the slow relaxation modes, respectively. The variable τ_{se} is some effective slow relaxation time, and the stretched exponent β ($0 < \beta \leq 1$) is an indication of the width of the distribution of relaxation times. In this work, the value of β depends on the hydrophobicity of the polymer and the level of surfactant addition. The mean slow relaxation time is given by

$$\tau_s \equiv \int_0^\infty \exp\left[-\left(\frac{t}{\tau_{se}}\right)^{\beta}\right] = \frac{\tau_{se}}{\beta}\Gamma\left(\frac{1}{\beta}\right) \qquad (2)$$

where $\Gamma(\beta^{-1})$ is the gamma function of β^{-1}.

The correlation functions were analyzed by using a nonlinear fitting algorithm (a modified Levenberg−Marquardt method) to obtain best-fit values of the parameters A_f, τ_f, τ_{se}, and β appearing on the right-hand side of eq 1. A fit was considered satisfactory if there were no systematic deviations in the plot of the residuals of the fitted curve.

Results and Discussion

Viscoelastic Properties. In Figure 2a, effects of the addition of surfactant on the dynamic viscosity η' at a low frequency of 0.01 Hz are depicted for the systems EHEC (1 wt %)/SDS, HM0-EHEC (1 wt %)/SDS, and HM4-EHEC (1 wt %)/SDS. A conspicuous feature for all the systems is that η' passes through a pronounced maximum for all systems, but the maximum is broader for the unmodified EHEC and located at a higher surfactant concentration (ca. 15 m*m*) than that of the hydrophobically modified polymers (ca. 4 m*m*). In the absence of surfactant, the value of η' is lowest for the unmodified EHEC and highest for the hydrophobically modified EHEC without spacer. This suggests that intermolecular hydrophobic associations between neighboring alkyl side chains play an important role even in solutions without surfactant. The fact that the dynamic viscosity of the HM0-EHEC solution without surfactant is significantly higher than that of the corresponding hydrophobically modified analogue with spacer (HM4-EHEC) may be ascribed to the higher flexibility of the side chains of the latter polymer. It is also possible that structural differences between the polymers, originating from a different distribution pattern of substituents along the cellulosic backbone, may contribute to this behavior. A blocky, inhomogeneous distribution of hydrophobic groups is expected to give an increase in viscosity. In this context we note that other research groups have reported on a difference of a spacer group on the viscosity of hydrophobically modified polymers. Hwang et al.[25] observed an enhancement in viscosity when a spacer was introduced. Tam et al.[26] found that the highest viscosity was obtained at an optimal spacer length. The findings were rationalized in terms of variation in strength of the micelles and a balance between intermolecular and intramolecular associations.

As is evident from Figure 2a, the dynamic viscosity for all systems is strongly dependent upon the level of surfactant addition, with at first an increase and then a decrease in the value of η'. The values of η', without and at low and moderate levels of SDS addition, are highest for the HM0-EHEC/SDS system, followed by those of the HM4-EHEC/SDS system, while the lowest values are observed for the unmodified EHEC. However, if we consider the relative change of η' by plotting the reduced dynamic viscosity $(\eta' - \eta'_0)/\eta'_0$, where η'_0 is the dynamic viscosity in the absence of surfactant, as a function of the SDS concentration (see the inset of Figure 2a), a different picture emerges. This procedure of analyzing data takes into account that the initial state of association is different for the three systems. In this framework, addition of SDS raises the reduced dynamic viscosity of the HM4-EHEC solution by a factor of 28, while the reduced viscosity is enhanced only by a factor of 15 for the corresponding HM0-EHEC solution. Note that the maximum increase in the reduced dynamic viscosity for the unmodified EHEC is approximately 10-fold, indicating that the relative change in polymer−surfactant interaction is not much affected by the incorporation of hydrophobic C12 and C14 alkyl chains. However, we should bear in mind that the unmodified EHEC (without any C12 and C14 alkyl chains) is also a polymer with hydrophilic and hydrophobic microdomains. The reduced viscosity shows that by introducing spacers in between the polymer backbone and the alkyl chains, the relative viscosity enhancement becomes considerably more accentuated (see the inset of Figure 2a). This effect can probably be attributed to the increased flexibility and length of the hydrophobic side chain, which should facilitate enhanced polymer−surfactant interaction.

When it comes to the difference in location between the maxima of η' (or the maxima of the reduced dynamic viscosity) for the systems containing hydrophobically modified polymers (with and without spacer) and the unmodified EHEC, this behavioral divergence can probably be rationalized in the following way. For the systems HM0-EHEC/SDS and HM4-EHEC/SDS it has been established[27,28] that SDS binds to the polymer at very low surfactant concentrations, while for EHEC/SDS the binding starts at a higher SDS concentration, the critical aggregation concentration. As a result of the different binding mechanisms, the maximum of η' is located at a lower SDS concentration for the hydrophobically modified EHEC samples than for the unmodified EHEC. The decrease in dynamic viscosity observed at higher levels of surfactant addition is attributed to a breakdown of the connectivity of the network as the hydrophobic groups of the polymer become saturated with surfactant.[29] At this stage, the effect of the polymer hydrophobic tails, which are present in a low number, is expected to gradually decrease with increasing surfactant concentration, and therefore the conjecture is that the interaction between surfactants and the backbone of HM0-EHEC or HM4-EHEC will approach that in the EHEC system. This situation, where the dynamic viscosity of the three systems is practically the same, seems to occur at a surfactant concentration of approximately 35 m*m* (see Figure 2a). We may also note that at high levels of surfactant addition the values of η' are significantly lower than the values of η' for the systems without surfactant. This indicates that high concentrations of SDS promote disruption of hydrophobic associations. At high SDS concentration, the surfactant also binds to the polymer backbone of HM4-EHEC and HM0-EHEC in the same way as to the unmodified EHEC. Thus, the polyelectrolyte effect is similar for the three polymers, and the rheology should only be dependent on the molecular weight of the polymers in the nonassociated stage. Therefore, the same value in viscosity indicates that the polymers have the same molecular weight as was observed from intensity light scattering experiments (see the Experimental Section) in dilute solutions of the polymers at a high level of surfactant addition.

In Figure 3, the dynamic storage and loss moduli are plotted as a function of frequency for 1 wt % aqueous solutions of EHEC, HM0-EHEC, and HM4-EHEC containing a moderate amount of SDS (4 m*m*). The EHEC/SDS system behaves approximately as a Newtonian liquid ($G' \sim \omega^2$ and $G'' \sim \omega^1$) over the considered frequency domain. The experimental scatter (at low frequencies) of the G' data for the EHEC/SDS system is probably due to the weak elastic response of this system (low viscous solution) at the considered surfactant concentration. The picture that emerges for these systems is that at low frequencies we observe a viscous behavior with $G'' > G'$, while at higher frequencies, depending on the level of surfactant addition, G' increases to cross G'', and above this frequency, G' exceeds G'', which suggests that the elastic response dominates. The frequency of intersection is located at low frequencies (long time of intersection) at surfactant conditions where the systems display strong polymer−surfactant interactions, while solutions of high levels of surfactant addition exhibit high frequencies of intersection.

The frequency dependencies of the dynamic moduli for simple systems can often be analyzed in the framework of the Maxwell model, which is the simplest model of a viscoelastic fluid. This model consists of an elastic component (spring) connected in series with a viscous component (dashpot). However, the Maxwell model could not, especially at strong polymer−surfactant interactions for the present systems, be used to ad-

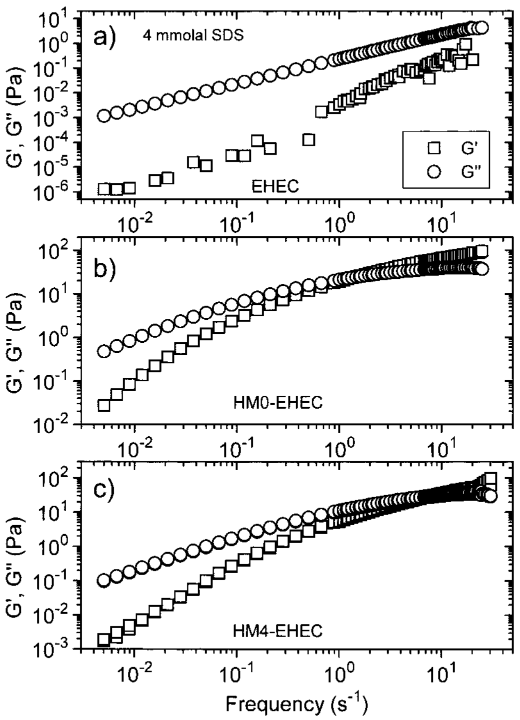

Figure 3. Frequency dependencies of the storage modulus (G') and the loss modulus (G'') for 1 wt % solutions at 4 m*m* SDS for EHEC (a), HM0-EHEC (b), and HM4-EHEC (c).

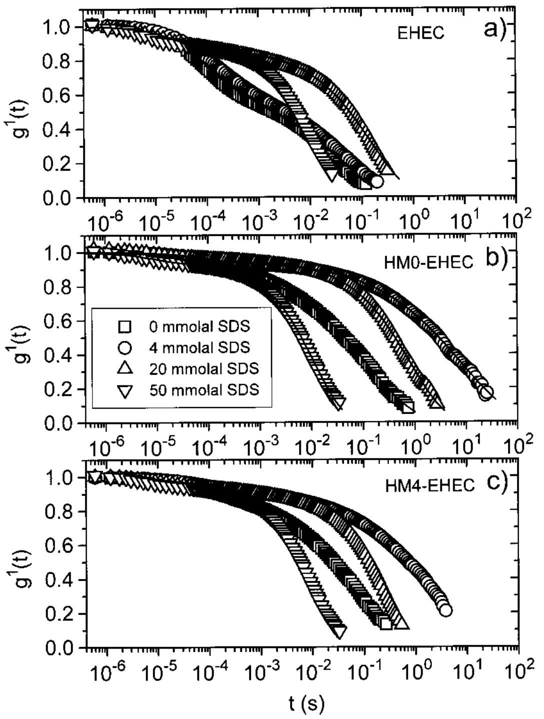

Figure 4. First-order electric field correlation function versus time (every third point is shown) for 1 wt % solutions of EHEC (a), HM0-EHEC (b), and HM4-EHEC (c) at the SDS concentrations indicated. The curves are fitted with the aid of eq 1.

equately describe the frequency dependencies of G' and G''. This observation suggests that the viscoelastic relaxation process is not controlled by a single relaxation time, but a more complex picture, with a broad distribution of relaxation times, emerges. We may note (cf. below) that the present DLS measurements yield a slow mode (the long-time tail of the correlation function) which is characterized by a distribution of relaxation times. The failure of the Maxwell model to describe rheological data of complex systems has previously been reported[11,12] for aqueous solutions of a hydrophobically modified EHEC and its unmodified analogue in the presence of a surfactant.

From results such as those in Figure 3, the quantity $\tau^* = 1/2\pi f^*$ is the time of intersection, or we may call it the longest time for the crossover point, and this time corresponds to the frequency of intersection f^* where G' equals G''. The longest relaxation time is associated with the lifetime of the transient network,[30] and the results in Figure 2b reveal the same characteristic features as those depicted in Figure 2a for the dynamic viscosity. As will be discussed below, this parameter exhibits a behavior that is reminiscent of that of the slow relaxation time obtained from dynamic light scattering.

Dynamic Light Scattering. Figure 4 shows correlation data at a scattering angle of 90° for the systems EHEC/SDS, HM0-EHEC/SDS, and HM4-EHEC at different levels of SDS addition. The correlation functions representing the HM0-EHEC/SDS system at various SDS concentrations have been fitted with the aid of eq 1 (solid curves). The time correlation function is always bimodal and can for all systems, at all levels of surfactant addition, initially be described by a single exponential (fast mode) followed by a stretched exponential (slow mode) at longer times. An inspection of the correlation functions for the HM0-EHEC/SDS and HM4-EHEC/SDS systems reveals that the slowing down of the long time relaxation process is strongest for the solutions with 4 m*m* SDS (close to the optimal value observed from the viscoelastic experiments) and weakest for the solutions with 50 m*m* SDS (low values of η' and τ^*). The shift in the relaxation time toward longer times is stronger for solutions containing the hydrophobically modified polymer without spacer than for those containing the polymer with spacer. This trend is consistent with the rheological features (cf. Figure 2b). The slowing down tendency is in general weakest for the EHEC/SDS system, and in this case the strongest slowing down is observed for the solution with 20 m*m* SDS (close to the optimum strength of polymer–surfactant interactions).

The effect of addition of SDS on the slow (τ_s) relaxation time of 1 wt % solutions of EHEC, HM0-EHEC, and HM4-EHEC, together with the rheological counterpart, is shown in Figure 5a. Although the slow relaxation times from DLS are considerably longer than the corresponding relaxation times from rheology, the pattern of behavior is similar with approximately the same location of the pronounced interaction peaks. This behavioral concordance suggests that the slow relaxation mode from DLS is associated with chain or cluster disengagement but that the relaxation processes from these different experimental methods may operate on different time scales. In view of these results, we may argue that the slow relaxation time can be used qualitatively to characterize differences in viscoelastic response between the systems.

The value of the stretched exponent β is a measure of the width of the distribution of relaxation times of the long-time tail of the time correlation function. A low value of β indicates a broad distribution of relaxation times. The effect of surfactant addition on the value of β is depicted for the unmodified and the hydrophobically modified EHEC systems in Figure 5b. For both the HM0-EHEC/SDS and HM4-EHEC/SDS systems β passes

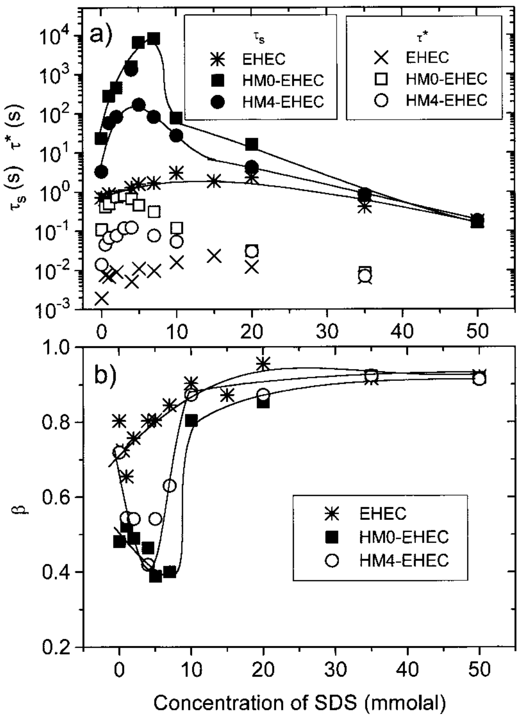

Figure 5. Effects of SDS concentration on the slow relaxation time τ_s and the time of intersection τ^* (a) and the stretched exponent β (b).

through a well-pronounced minimum, which is located at the SDS concentration where the viscosity enhancement of the system is highest. In the case of the EHEC/SDS system, the value of β rises at low and moderate SDS concentrations and β assumes gradually a constant value (approximately 0.9) at high surfactant concentrations. We may note that at high levels of surfactant addition β is large and virtually the same for the three systems. These results can be rationalized in the framework of the coupling approach of Ngai.[24,31]

In this coupling model, which provides a general description of the dynamics in constrained and interacting systems,[32] the value of β or the value of the coupling parameter n ($\beta = 1 - n$) is a direct measure of the coupling strength of the relaxation mode to its complex environments. A high value of n or a low value of β indicates strong coupling effects. Although the general derivation of the coupling model for complex systems from first principles is not known yet, this approach has shown to be powerful in the analysis of various dynamical features of polymer systems. The model treats the system under consideration as a combination of "basic units" that interact nonlinearly with each other. The coupling model recognizes short and long time domains that are separated by a crossover time t_c. At short times ($t < t_c$) "basic units" relax independently; their relaxation is characterized by a temporal correlation function (an example is the field autocorrelation function) of the general form

$$\phi(t) = \exp(-t/\tau_0) \qquad t < t_c \tag{3}$$

where τ_0 is the characteristic time for unconstrained relaxation, and this quantity exhibits a q^2 dependence. At $t > t_c$, cooperative constrains between the "basic units" come into play. In this case the relaxation function $\phi(t)$ depends on the coupling strength ($0 \leq n < 1$) between basic units, so that this function is characterized by the slowed stretched exponential function

$$\phi(t) = \exp[-(t/\tau_s^*)^{1-n}] \qquad t > t_c \tag{4}$$

Here τ_s^* is the characteristic time for constrained relaxations. The basic prediction of this model is that n rises (or β decreases) as the strength of the interaction between the basic units is increased. A continuity condition on $\phi(t)$ at $t = t_c$ yields

$$\tau_s^* = [t_c^{-n}\tau_0]^{1/1-n} \tag{5}$$

This relationship links the effective relaxation time τ_s^* to the independent relaxation time τ_0 and the crossover time t_c.

In view of the coupling model, the observed effects of surfactant addition on the stretched exponent β (Figure 5b) and on the slow relaxation time (Figure 5a) can be rationalized. The fact that the intermolecular hydrophobic interactions are strengthened at moderate levels of surfactant addition for the HM0-EHEC/SDS and HM4-EHEC/SDS systems should, in terms of the coupling model, imply that the coupling strength increases. The predictions from the coupling model under these conditions are that β drops, and the slow relaxation time should increase (see eq 5) with decreasing β. These predictions are both in accordance with the experimental findings (see Figure 5). At high surfactant concentrations, where the polymer–polymer hydrophobic interactions are disturbed by the high surfactant binding to the polymer, the coupling strength or the intermolecular interactions should be diminished, and we expect that β rises and the slow relaxation time falls off. These predictions are consistent with the experimental observations.

The angular dependence of the correlation function, for the HM4-EHEC/SDS system at different levels of surfactant addition, is illustrated in the form of a reduced plot in Figure 6. The same type of behavior is also observed for the other two polymer–surfactant systems. The general trend is that correlation function data practically condense onto a single curve at short times, reflecting the diffusive character (q^2-dependent) of the fast mode, while the long-time tails of the correlation functions are more or less separated, depending on the surfactant concentration, indicating a q dependence stronger than that of a diffusive process. A quantitative determination of the complex q dependence of the slow mode is given below.

The q dependence of inverse slow relaxation time may be expressed as $\tau_s^{-1} \propto q^{\alpha_s}$, and in Figure 7a a plot of this type has been constructed for the HM0-EHEC/SDS system in the presence of different amounts of surfactant. It is obvious that the angular dependence of the slow mode is a function of the level of SDS addition. Actually, the strongest q dependence of the slow mode is observed at the surfactant concentrations where the systems have their respective optimum in polymer–surfactant interaction (see Figure 7b). A strong angular dependence of the slow relaxation mode has previously been interpreted as arising from large clusters of various sizes or the presence of large-scale "heterogeneities".[33−35] Several DLS studies[11,18,20,22,36−39] on associating polymer systems and gelling systems have revealed that the q dependence of the slow mode is stronger than that of the fast mode.

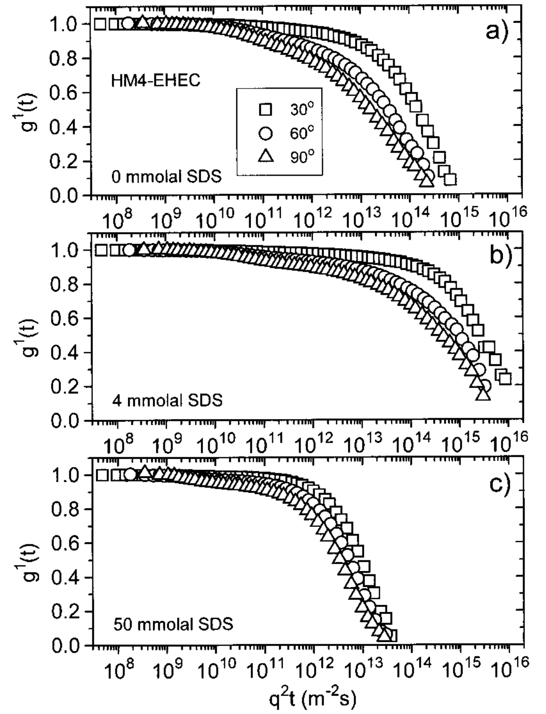

Figure 6. Plot of the first-order electric field correlation function versus q^2t (every third point is shown) for 1 wt % solutions of HM4-EHEC at the SDS concentrations indicated.

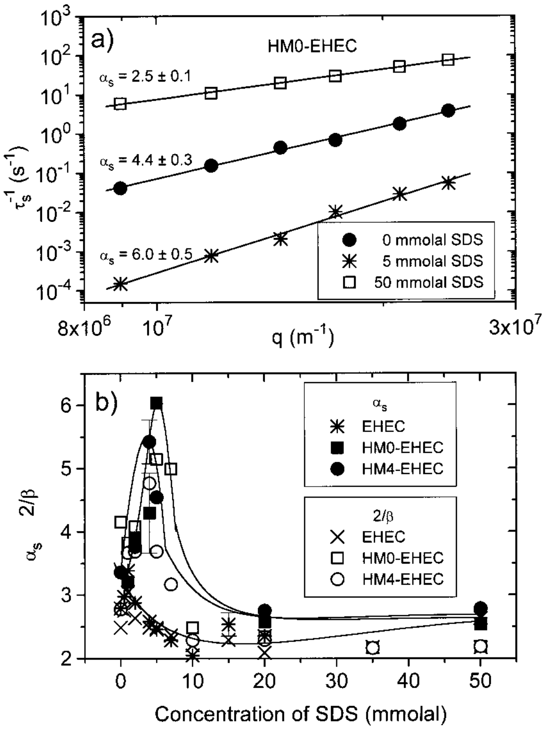

Figure 7. (a) Illustration of the wave vector dependence of the slow (τ_s^{-1}) inverse relaxation times for HM0-EHEC at the surfactant concentrations indicated. (b) Effect of SDS concentration on the quantities $2/\beta$ (see main text for explanation) and α_s, illustrating the q dependence of the slow inverse relaxation mode.

Another unique feature of the coupling model is that it predicts[24] the q dependence of the slow relaxation time through the relationship

$$\tau_s^*(q) = [t_c^{-n}\tau_0(q)]^{1/(1-n)} \propto q^{-2/(1-n)} \propto q^{-2/\beta} \qquad (6)$$

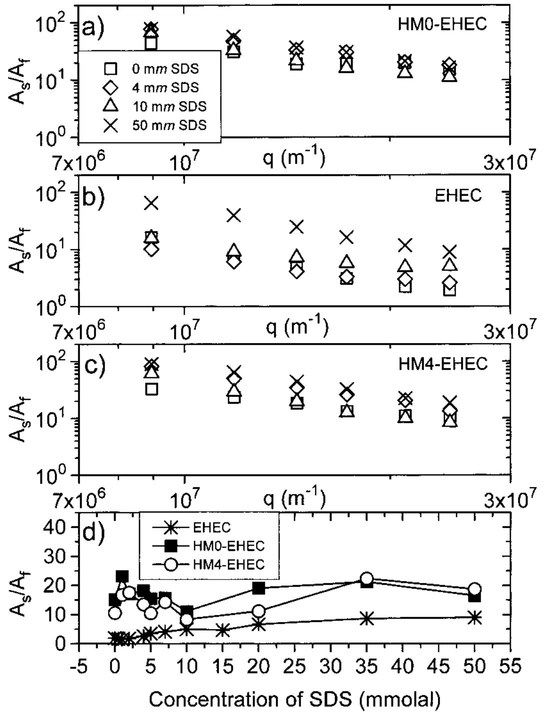

Figure 8. (a–c) Wave vector dependence of the reduced amplitude for the polymers and surfactant concentrations indicated. (d) Effect of SDS concentration on the reduced amplitude.

Since the characteristic time for unconstrained relaxation τ_0 is diffusive ($\tau_0(q) \propto q^{-2}$), a stronger q dependence of the slow relaxation time is predicted if there is coupling effects, that is, $\beta < 1$. In the case of enhanced interactions, as the above-discussed surfactant-induced interactions, we expect a concomitant increase in the coupling parameter n, or a decrease of β, and a stronger q dependence of the slow relaxation time. The q dependence of the slow mode is illustrated in Figure 7b, where the values of α_s and the predicted values ($2/\beta$) are plotted as a function of surfactant concentration. Although the numerical agreement between the experimental and calculated values is not perfect, the trends of the systems are well captured.

The q dependence of the reduced amplitude (A_s/A_f) for solutions of EHEC, HM0-EHEC, and HM4-EHEC containing different amounts of SDS is shown in Figure 8a–c. The general picture that emerges at all conditions is the increase of the ratio as the value of q decreases. This trend, which indicates the existence of large clusters, suggests the presence of large aggregates even at high levels of surfactant addition. A conspicuous feature in Figure 8b for the EHEC–SDS system is that the values of the reduced amplitude, over the considered q range, are significantly higher at 50 mm SDS than the corresponding values of the ratio at lower surfactant concentrations.

The effect of surfactant addition on the reduced amplitude is further illustrated in Figure 8d, where the ratio (at a scattering angle of 90°) is plotted as a function of SDS concentration for the three polymer–surfactant systems. It should be mentioned that although the numerical values of the ratio are angular dependent, the ratios of the systems exhibit the same pattern of behavior at the considered scattering angles upon SDS addition. For the EHEC–SDS system, we observe a progressive rise of A_s/A_f with increasing SDS concentra-

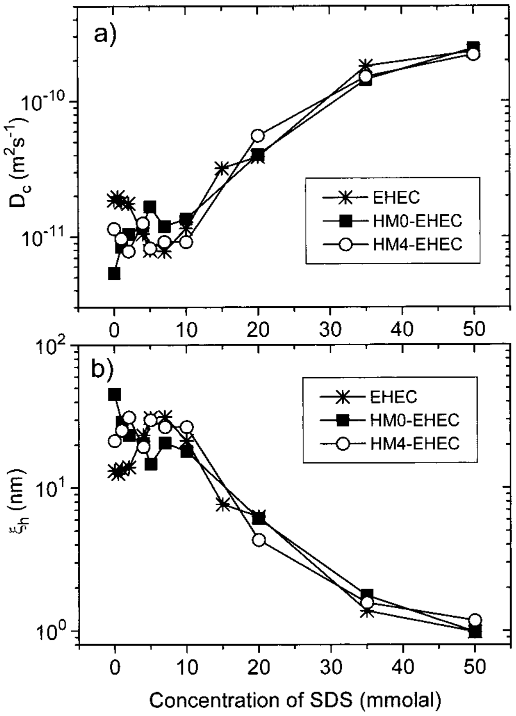

Figure 9. Effect of SDS concentration on the cooperative diffusion coefficient (a) and the hydrodynamic correlation length ξ_h (b).

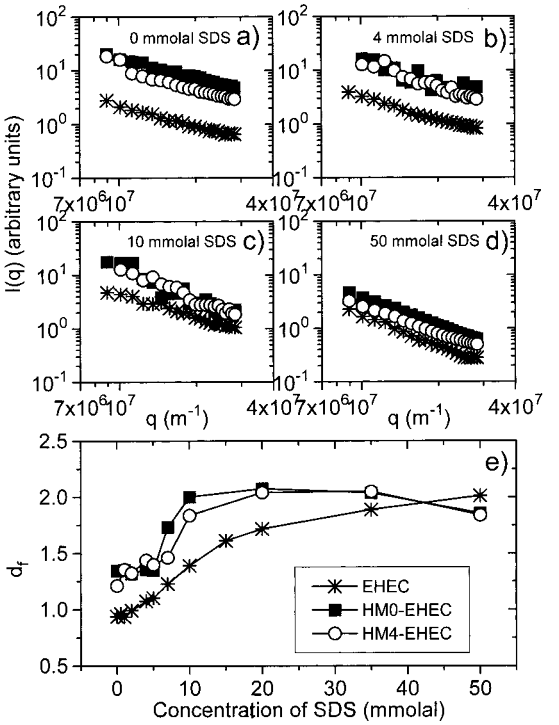

Figure 10. (a–d) Log–log plots of the q dependence of the scattered intensity for the polymers and surfactant concentrations indicated. (e) Effect of surfactant concentration on the fractal dimension (see eq 7).

tion. A rise of the ratio is also observed for the HM0-EHEC/SDS and HM4-EHEC/SDS systems at surfactant concentrations above 10 m*m*. However, for the hydrophobically modified polymers there is indication of peaks at moderate SDS concentrations, where a pronounced viscosity enhancement occurs for these systems. Intuitively, one would expect that the contribution of the amplitude of the slow mode should diminish due to weaker associations at higher surfactant concentrations. However, the picture may be more intricate due to polyelectrolyte effects of these systems. In this context it may be interesting to note a recent light scattering study[40] on polyelectrolyte solutions, where a fast and a slow relaxation mode were observed in the decay of the correlation function. A complex interplay between the amplitudes of the fast and the slow mode was reported. It was shown that the amplitudes of both the fast and the slow modes respond to electrostatic interactions, each in a different way. The amplitude of the slow mode was found to be sensitive to charge interaction parameters such as ionic strength of the solution. The present polymer–surfactant systems possess polyelectrolytic character, and in this type of mixture, involving an ionic surfactant, it has been found[29] that the free surfactant often dominates and gives important contributions to the ionic strength. Our conjecture is that a change of the electrostatic interactions with surfactant addition may contribute to the observed feature of the ratio at higher surfactant concentrations.

The fast relaxation mode ($\tau_f^{-1} = D_c q^2$) is diffusive for all systems at all conditions and yields the cooperative diffusion coefficient D_c. The effect of surfactant addition on D_c for 1 wt % solutions of the systems EHEC/SDS, HM0-EHEC/SDS, and HM4-EHEC/SDS is depicted in Figure 9a. The behavior of the cooperative diffusion coefficient is similar for the three systems, at least at higher levels of surfactant addition, with increasing values of D_c at higher surfactant concentrations. This diffusion process is governed by the interplay between hydrodynamic and thermodynamic properties through the expression[41] $D_c \cong s\,\partial\Pi/\partial c$, where s is the sedimentation coefficient and $\partial\Pi/\partial c$ is the inverse osmotic compressibility. In light of this relationship, the conjecture is that the thermodynamic factor ($\partial\Pi/\partial c$) dominates, and D_c rises due to the gradually improved thermodynamic conditions (increasing values of $\partial\Pi/\partial c$) of the systems[42] with increasing amount of surfactant.

In the framework of the "blob" model for semidilute solutions, a cooperative diffusion coefficient associated with network deformations can be defined by[41] $D_c \propto k_B T/6\pi\eta_0\xi_h$, where k_B is Boltzmann's constant, T is the absolute temperature, η_0 is the solvent viscosity, and ξ_h is the dynamic screening length. The latter quantity can be viewed as a characteristic mesh size of the transient network. The general picture that emerges from Figure 9b is that the mesh size decreases as the surfactant concentration increases, and no obvious difference in behavior between the three systems can be detected at higher levels of surfactant addition. This decrease may be rationalized in the following scenario. At low surfactant concentrations, where strong polymer–polymer hydrophobic associations persist in the systems, a heterogeneous network containing bundles of close-packed chains is formed, and as a result, the effective mesh size of the network becomes large. As the level of surfactant addition increases, the bundles are progressively disrupted, and the polymer network undergoes a gradual structural reorganization to a more homogeneous structure (see Figure 11). In this process the average mesh size of the network is expected to decrease. The correlation length calculated with the aid of the equation above yields a value of about 1 nm at high surfactant concentrations. This is a very low value of ξ_h, but we should bear in mind that the factor 6π in the above equation has no precise meaning[41] but is a

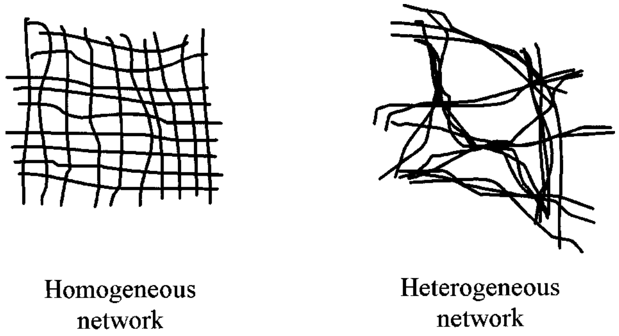

Figure 11. Illustration of the structural reorganization of the polymer network from homogeneous (high SDS concentrations) to heterogeneous (low SDS concentrations). In the latter stage, bundles of polymer chains are formed in the network, and the average spacing between bundles are larger than the average mesh size of the homogeneous network.

convenient reminder of the similarity with the Stokes law for viscous motion of a sphere. Therefore, we should not pay too much attention to the numerical value of ξ_h, but rather on the relative change of this parameter with surfactant addition.

A close inspection of the correlation length data for the EHEC−SDS system reveals a maximum at moderate surfactant concentrations, while no pronounced peak can be discerned for the hydrophobically modified polymers. One may argue that the tendency of forming bundles should first rise as SDS is added in the low surfactant concentration regime, reach a maximum, and then decrease as the bundles are gradually disrupted and a more homogeneous network is evolved. This scenario suggests that the correlation length should initially rise at low surfactant concentrations, attain a maximum, and then decrease. This trend is consistent with the feature observed for the EHEC−SDS system. A reasonable conjecture is that this effect is associated with the onset of surfactant binding to the polymer (cac). The value of cac is about 3 m*m*[28] for the EHEC−SDS system, which is not far away from the location of the maximum in Figure 9b. When it comes to the hydrophobically modified analogues, the onset of surfactant binding to the polymer occurs at a much lower surfactant concentration.[28] It is possible that the optimum of bundle formation occurs at very low levels of SDS addition for the HM0-EHEC and HM4-EHEC systems so that the maximum is not visible at the SDS concentrations considered here. We may note that, in the absence of SDS and at low surfactant concentrations, ξ_h is larger for the systems containing the hydrophobically modified polymers.

Intensity Light Scattering. To obtain further information about the network structure, we may use intensity light scattering to probe the local structural properties of the systems. If we consider the systems in the regime $q\xi_s > 1$, the length scale q^{-1} is related to local properties, and the scattered intensity depends strongly on the length scale. In this regime, a semidilute solution can be viewed as an irregular fractal network,[43] formed by more or less interpenetrating clusters. In this case the scattering intensity decays with the wave vector as

$$I(q) \propto q^{-d_f} \tag{7}$$

where the slope of the scattered intensity in the power-law region yields the fractal dimension d_f.

Figure 10a−d shows the intensity profiles in form of log−log plots of the scattered intensity versus q for 1 wt % solutions of EHEC, HM0-EHEC, and HM4-EHEC in the presence of different amounts of SDS. We can see that the scattered intensities for the solutions containing the hydrophobically modified polymers at low surfactant concentrations are significantly higher than for the intensities of the corresponding EHEC solutions, while at higher levels of SDS addition this difference disappears. This is probably another manifestation of strong associations of the hydrophobically modified polymers, giving rise to large domains with high scattering ability.

The effect of surfactant addition on the fractal dimension for 1 wt % solutions of EHEC, HM0-EHEC, and HM4-EHEC is depicted in Figure 10e. The values of d_f are, except at the highest surfactant concentration, higher for the hydrophobically modified polymers than the corresponding ones for the unmodified EHEC. This suggests that the networks formed from the hydrophobically modified polymers are more “tight”, which may be due to branching effects of the HM0-EHEC and HM4-EHEC networks. The rise of d_f with increasing SDS concentration, a common feature for the three polymer systems, indicates that the networks undergo structural reorganizations from “open” to more “tight” networks[44] as the amount of added surfactant increases. This is consistent with the picture discussed above. The scenario outlined above is reminiscent of a recent model[45,46] developed to describe the temperature-induced gelation of EHEC−surfactant systems.

Acknowledgment. We thank Akzo Nobel Surface Chemistry AB for supplying the polymer samples. S.N. and K.T. also thank the Centre of Competence for Amphiphilic Polymers (CAP) for financial support. The rheometer was funded by a grant from Nils and Dorthi Troëdsson’s Research Foundation. We thank an anonymous referee for valuable comments.

References and Notes

(1) Glass, J. E., Ed. *Polymers in Aqueous Media*; American Chemical Society: Washington, DC, 1989; Vol. 223.
(2) McCormick, C. L.; Bock, J.; Schulz, D. N. Water-soluble Polymers. In *Encyclopedia of Polymer Science and Engineering*; Mark, H. F., Bikales, N. M., Overberger, C. G., Menges, G., Eds.; Wiley-Interscience: New York, 1989; Vol. 17, pp 730−784.
(3) Schulz, D. N., Glass, J. E., Eds. *Polymers as Rheology Modifiers*; American Chemical Society: Washington, DC, 1991.
(4) Dubin, P., Bock, J., Davies, R. M., Schulz, D. N., Thies, C., Eds. *Macromolecular Complexes in Chemistry and Biology*; Springer-Verlag: Berlin, 1994.
(5) Kwak, J. C. T., Ed. *Polymer-surfactant Systems*; Marcel Dekker: New York, 1998; Vol. 77.
(6) Tanaka, R.; Meadows, J.; Williams, P. A.; Phillips, G. O. *Macromolecules* **1992**, *25*, 1304.
(7) Thuresson, K.; Nilsson, S.; Lindman, B. *Langmuir* **1996**, *12*, 2412.
(8) Kjøniksen, A.-L.; Nyström, B.; Lindman, B. *Macromolecules* **1998**, *31*, 1852.
(9) Nilsson, S.; Thuresson, K.; Hansson, P.; Lindman, B. *J. Phys. Chem. B* **1998**, *102*, 7099.
(10) Thuresson, K.; Nyström, B.; Wang, G.; Lindman, B. *Langmuir* **1995**, *11*, 3730.
(11) Nyström, B.; Thuresson, K.; Lindman, B. *Langmuir* **1995**, *11*, 1994.
(12) Thuresson, K.; Lindman, B.; Nyström, B. *J. Phys. Chem. B* **1997**, *101*, 6450.
(13) Kjøniksen, A.-L. Unpublished results.
(14) Thuresson, K.; Karlström, G.; Lindman, B. *J. Phys. Chem.* **1995**, *99*, 3823.

(15) Chu, B.; Onclin, M.; Ford, J. R. *J. Phys. Chem.* **1984**, *88*, 6566.
(16) Guinier, A.; Fournet, G. *Small Angle Scattering of X-rays*; J. Wiley & Sons: New York, 1955.
(17) Martin, J. E.; Wilcoxon, J.; Odinek, J. *Phys. Rev. A* **1991**, *43*, 858.
(18) Nyström, B.; Roots, J.; Carlsson, A.; Lindman, B. *Polymer* **1992**, *33*, 2875.
(19) Wang, C. H.; Zhang, X. Q. *Macromolecules* **1993**, *26*, 707.
(20) Nyström, B.; Walderhaug, H.; Hansen, F. K. *J. Phys. Chem.* **1993**, *97*, 7743.
(21) Raspaud, E.; Lairez, D.; Adam, M.; Carton, J.-P. *Macromolecules* **1994**, *27*, 2956.
(22) Nyström, B.; Lindman, B. *Macromolecules* **1995**, *28*, 967.
(23) Douglas, J. F.; Hubbard, J. B. *Macromolecules* **1991**, *24*, 3163.
(24) Ngai, K. L. *Adv. Colloid Interface Sci.* **1996**, *64*, 1.
(25) Hwang, F. S.; Hogen-Esch, T. E. *Macromolecules* **1995**, *28*, 3328.
(26) Tam, K. C.; Farmer, M. L.; Jenkins, R. D.; Basset, D. R. *J. Polym. Sci. B* **1998**, *36*, 2275.
(27) Thuresson, K.; Söderman, O.; Hansson, P.; Wang, G. *J. Phys. Chem.* **1996**, *100*, 4909.
(28) Nilsson, S.; Thuresson, K.; Nyström, B.; Lindman, B. Manuscript in preparation.
(29) Piculell, L.; Guillemet, F.; Thuresson, K.; Shubin, V.; Ericsson, O. *Adv. Colloid Interface Sci.* **1996**, *63*, 1.
(30) Rubinstein, M.; Dobrynin, A. V. *Trends Polym. Sci.* **1987**, *5*, 181.
(31) Ngai, K. L.; Rendell, R. W. *Philos. Mag. B* **1998**, *77*, 621.
(32) Ngai, K. L.; Phillies, G. D. J. *J. Chem. Phys.* **1996**, *105*, 8385.
(33) Richtering, W.; Löffler, R.; Burchard, W. *Macromolecules* **1992**, *25*, 3642.
(34) Richtering, W.; Gleim, W.; Burchard, W. *Macromolecules* **1992**, *25*, 3795.
(35) Bodycomb, J.; Hara, M. *Macromolecules* **1995**, *28*, 8190.
(36) Ren, S. Z.; Sorensen, C. M. *Phys. Rev. Lett.* **1993**, *70*, 1727.
(37) Konak, C.; Helmstedt, M.; Bansil, R. *Macromolecules* **1997**, *30*, 4342.
(38) Thuresson, K.; Nilsson, S.; Kjøniksen, A.-L.; Walderhaug, H.; Lindman, B.; Nyström, B. *J. Phys. Chem. B* **1999**, *103*, 1425.
(39) Tsianou, M.; Kjøniksen, A.-L.; Thuresson, K.; Nyström, B. *Macromolecules* **1999**, *32*, 2974.
(40) Sedlák, M. *J. Chem. Phys.* **1996**, *105*, 10123; *Langmuir* **1999**, *15*, 4045.
(41) De Gennes, P.-G. *Scaling Concepts in Polymer Physics*; Cornell University Press: Ithaca, NY, 1979.
(42) Thuresson, K.; Lindman, B. *J. Phys. Chem. B* **1997**, *101*, 6460.
(43) Daoud, M.; Leibler, L. *Macromolecules* **1988**, *21*, 1497.
(44) Muthukumar, M. *Macromolecules* **1989**, *22*, 4656.
(45) Cabane, B.; Lindell, K.; Engström, S.; Lindman, B. *Macromolecules* **1996**, *29*, 3188.
(46) Lindell, K.; Cabane, B. *Langmuir* **1998**, *14*, 6361.

MA9911391